Uranium-series isotope and thermal constraints on the rate and depth of silicic magma genesis

A. DOSSETO[1], S. P. TURNER[1], M. SANDIFORD[2] & J. DAVIDSON[3]

[1]*GEMOC National Key Centre, Department of Earth and Planetary Sciences, Macquarie University, Sydney, NSW 2109, Australia (e-mail: adosseto@els.mq.edu.au)*

[2]*School of Earth Sciences, University of Melbourne, Melbourne VIC 3010, Australia*

[3]*Department of Earth Sciences, University of Durham, South Road, Durham DH1 3LE, UK*

Abstract: Uranium-series isotopes provide important constraints on the timescale of magma differentiation and this can be used to identify where in the crust and silicic magmas acquire their geochemical characteristics. Timescales of differentiation can be inferred from the observed co-variations of U-series disequilibria with differentiation indexes. When crustal assimilation of secular equilibrium material is involved, inferred timescales will generally decrease. In turn, they will increase if periodical recharge (>20 wt% relative volume) of the magma body occurs. If crustal assimilation and magma recharge occur concurrently, inferred timescales for differentiation can be similar to that of closed system differentiation. We illustrate the approach with data from Mount St Helens which suggest that dacitic compositions are produced in *c*. 2000 years. Combining this with recent evidence for an important role for amphibole fractionation suggests that differentiation of a *c*. 10 km^3 magma body at this volcanic centre occurs at 8–10 km depth in the crust.

The genesis of silicic magmas is important for understanding the growth of the continental crust and the origin of explosive eruptions because the upper crust is dominated by silicic igneous rocks, and evolved lavas are responsible for many of the most dangerous volcanic eruptions. Over the last two decades, numerous efforts have been undertaken to constrain how and where silicic magmas are generated (e.g. Davidson 1985; Huppert & Sparks 1988; Bergantz 1989; Bergantz & Dawes 1992; Laube & Springer 1998; Petford & Gallagher 2001; Orozco-Esquivel *et al.* 2002; Annen & Sparks 2002; Annen *et al.* 2006). In particular, recent thermal modelling has shown that repetitive intrusions of basalt can melt pre-existing intrusions in the lower crust and that the combination of residual magmas from basalt crystallization and these crust-derived melts in a deep crustal hot zone could produce silicic magmas and account for observed compositional variations in silicic volcanic systems (Annen & Sparks 2002; Annen *et al.* 2006). However, the timescales of magma differentiation can also be used to constrain the depth where silicic magmas acquire their geochemical characteristics and thus provide an important test of these models. An important aspect of the model of Annen *et al.* (2006) is that, whilst silicic magmas can be produced rapidly as the residue of basalt crystallization, the timescales for large volumes of melt to accumulate by melting of the crust are very long (*c*. 100 ka).

One constraint upon the timescales and relative proportions of liquid derived from recently emplaced basalt v. crustal melt in these hot zone models is that most silicic arc magmas contain significant $^{230}Th/^{238}U$ and $^{226}Ra/^{230}Th$ disequilibria (Cooper & Reid 2003; Turner *et al.* 2003*a*, *b* for a recent compilation). These disequilibria are believed to be derived from slab fluids (Turner *et al.* 2001; Bourdon *et al.* 2003). Thus, in order to preserve radioactive disequilibria, significantly less than 8 ka (five half-lives of ^{226}Ra) can elapse during the evolution from mantle-derived basalts to andesitic and dacitic compositions and their eruption. Moreover, many suites of rocks from individual volcanoes show a correlated decrease in ($^{226}Ra/^{230}Th$) with increasing differentiation (as measured by SiO_2 or Th content). This has been taken to indicate that differentiation occurred over a timescale proportional to the half-life of ^{226}Ra and detailed studies have used the change in ($^{226}Ra/^{230}Th$) to infer the timescale in detail (e.g. Turner *et al.* 2003*a*, *b*; George *et al.* 2004). In this case, the silicic rocks must derive their geochemical characteristics almost entirely from crystallization of a single sill of basalt. Consequently, there is a need for a model that accounts for both the rapid generation of silicic magmas (in order to preserve Ra–Th disequilibrium) and their geochemical and isotopic diversity and evidence for crustal assimilation in many instances (e.g. Smith & Leeman 1987; Grove *et al.* 1988; Tepper *et al.* 1993; Bourdon

From: ANNEN, C. & ZELLMER, G. F. (eds) *Dynamics of Crustal Magma Transfer, Storage and Differentiation*. Geological Society, London, Special Publications, **304**, 169–181.
DOI: 10.1144/SP304.9 0305-8719/08/$15.00

et al. 2000). Moreover, if andesites are directly derived from crystallization of a basaltic sill, this requires no contribution from residual melts of previously crystallized intrusion.

A second issue is that hydrous basalt cooling in the mid- to lower crust will crystallize amphibole and partial melts of earlier intruded basalt will probably form in the presence of residual amphibole. Thus, it now appears that amphibole fractionation may play a more critical role in the compositional evolution of arc magmas than the gabbroic assemblages with which they typically erupt (Davidson *et al.* 2007). Radium can be moderately compatible in amphibole (Blundy & Wood 2003) and so there is also a need to appraise the effects of amphibole fractionation on ^{226}Ra disequilibria and to reconsider how this may affect our inferences about the timescales of differentiation.

Accordingly, we have explored two end-member models. In the first, the radioactive disequilibrium in andesites and dacites is largely derived from zero-aged basalt mixed with crustal and residual melts just before eruption, since mixing has the potential to be an important process for the production of some intermediate silicic rocks (Zellmer *et al.* 2005). In the second model, crustal and residual melts are mixed with a primary basaltic magma during crystallization (assimilation-fractional crystallization). The role of amphibole fractionation during this assimilation-fractional crystallization has also been assessed.

Model I: mixing of zero-aged basalt with crustal and residual melts just before eruption

One end-member model to account for the geochemical characteristics of andesitic and dacitic magmas involves mixing of high-silica melts with 'zero-aged' basalt that imparts mantle-derived U-series disequilibria to the hybrid magma. Eruption takes place less than a few hundreds of years after mixing in order that Ra–Th disequilibrium is preserved. The high-silica melts are derived from a combination of partial melting of the crust and the residues of crystallization of the most recent magmatic intrusions. Annen & Sparks (2002) suggested that high-silica melts are produced in a significant volume only after successive magma emplacements over $>10^5$ years. In this case, the crustal melts will be in secular equilibrium for the $^{238}U/^{230}Th/^{226}Ra$ systems. Secondly, these crustal melts are produced by partial melting of amphibolite (Annen *et al.* 2006). Berlo *et al.* (2004) have shown that partial melting of amphibolite is unlikely to produce significant radioactive disequilibrium and so any observed disequilibria must be inherited from the 'zero-aged' basalt. Dufek & Cooper (2005) suggested that it might be possible to produce ^{226}Ra excess during continuous dehydration melting of the lower crust. However, this model cannot account for the positive correlation between ($^{226}Ra/^{230}Th$) and Sr–Th ratios often observed in arc lavas (Dosseto *et al.* 2003).

In order to quantify the contribution of zero-aged basalt required in the mixing model described above, we use the average composition of subduction-related andesites and dacites for which SiO_2, U, ^{226}Ra contents, ($^{238}U/^{230}Th$) and ($^{226}Ra/^{230}Th$) data are available ($n=36$) and calculate the proportion of zero-aged basalt and the composition of zero-aged basalt and high-silica melt end-member that best reproduce this average andesite/dacite composition. The range of possible values for the SiO_2 and U contents of the high-silica melt is 59–73 wt% and 1.5–4.5 ppm, respectively (average upper continental crust; Taylor & McLennan 1995), whereas for the SiO_2 content of the zero-aged basalt it is 48–52 wt% (average composition of subduction-related basalts measured for $^{238}U/^{230}Th/^{226}Ra$; $n=51$). The range of possible values for the U content of the basalt end-members is 0.01–4 ppm, which is the range exhibited by subduction-related basalts for which combined $^{238}U/^{230}Th/^{226}Ra$ data are available. Three models were considered. In model Ia, the range of possible values for the ($^{238}U/^{230}Th$) and ($^{226}Ra/^{230}Th$) activity ratios of the basalt is simply the average values for subduction-related basalts: 1.1 ± 0.2 and 2 ± 1, respectively (1 standard deviation). In model Ib, the ($^{238}U/^{230}Th$) and ($^{226}Ra/^{230}Th$) activity ratios of the basalt are extreme values corresponding to theoretical compositions for slab-derived fluids: 8 and 17, respectively (Turner *et al.* 2003*a*, *b*). In these two models, activity ratios for the high-silica end-member are taken equal to unity (secular equilibrium) as explained above. In model Ic, the parental basalt is the same as that of model Ia but the high-silica melt has been allowed to have some radioactive disequilibria: ($^{238}U/^{230}Th$)=($^{226}Ra/^{230}Th$)=1.2, those being the maximum values calculated by Berlo *et al.* (2004) for an amphibolitic melt.

Starting compositions of the zero-aged basalt and silicic melt are compiled in Table 1 and results of the inversion are shown in Table 2 and Figure 1. Inversion of the average arc andesite/dacite composition yields a SiO_2 composition of the zero-aged basalt and the crustal melt at the higher end of the allowed range of values for all three models. As a consequence, because mixing end-members always have the same SiO_2 content regardless of their activity ratios, mixing proportions are controlled by the SiO_2 content of the end-member magmas.

Table 1. *Range of values allowed for the two components in the mixing models*

	Model 1	Model 2	Model 3
SiO_2 high-silica melt (wt%)	59–73	59–73	59–73
SiO_2 zero-aged basalt (wt%)	48–52	48–52	48–52
U high-silica melt (ppm)	1.5–4.5	1–5	1–5
U zero-aged basalt (ppm)	0.01–4	0.01–4	0.01–4
$(^{238}U/^{230}Th)$ high-silica melt	1	1	1.2
$(^{238}U/^{230}Th)$ zero-aged basalt	0.9–1.3	8	0.9–1.3
$(^{226}Ra/^{230}Th)$ high-silica melt	1	1	1.2
$(^{226}Ra/^{230}Th)$ zero-aged basalt	1–3	17	1–3

See text for explanation of the chosen component compositions.

For all three models, the U-series composition of an average arc andesite/dacite can be explained by the mixture between *c*. 45% of pre-existing silicic crustal melt (produced through basalt crystallization and/or wallrock melting) and *c*. 55% of zero-age basaltic magma. Sparks & Marshall (1986) showed that complete magma hybridization is only possible with proportions of mafic magma greater than 50%, which is the case here.

However, this model assumes magma mixing without any requirement for crystal fractionation to occur. This is at odds with the numerous studies which have observed that the geochemistry of silicic lavas is at least partially controlled by crystal fractionation (Grove & Kinzler 1986 and references therein). For instance, this process is unable to explain the curvilinear trends so often observed between the abundance of elements such as TiO_2 or P_2O_5 and differentiation index (Turner *et al.* 2003*a*, *b*; George *et al.* 2004; Zellmer *et al.* 2005). Therefore, in the following section, we consider more realistic model of coupled assimilation-fractional crystallization (AFC). The effect of crustal assimilation, magma recharge and amphibole fractionation on U-series-derived timescales for magma differentiation is then evaluated.

Model II: assimilation of crustal/residual melts during differentiation ± magma recharge

Assimilation of secular equilibrium materials will act to reduce $(^{226}Ra/^{230}Th)$ ratios, mimicking the effects of time and associated radioactive decay. Consequently, the magma differentiation timescale inferred from a specific dataset will represent maxima unless assimilation (which must be independently established) is quantitatively taken into account. In this section, we investigate quantitatively the effect of crustal assimilation during differentiation on timescales inferred from Ra–Th data. To illustrate this, we use U-series data from Mount St Helens (Fig. 2; Volpe & Hammond 1991), where the operation of AFC has been demonstrated (Halliday *et al.* 1983). Note that the objective of this discussion is not to re-appraise previous U-series interpretations (Volpe & Hammond 1991; Cooper & Reid 2003). Calculations performed for other volcanoes (e.g. Ruapehu, New Zealand, Price *et al.* 2007; Sangeang Api, Indonesia) yield similar conclusions to that presented below. We focused on whole-rock Ra–Th data, as it has been shown

Table 2. *Results of the numerical modelling of mixing processes*

	Model 1	Model 2	Model 3
X_{basalt} (%)	55.6 ± 0.1	54 ± 5	55 ± 2
SiO_2 high-silica melt (wt%)	72.94 ± 0.03	73 ± 1	73.0 ± 0.9
SiO_2 zero-aged basalt (wt%)	51.97 ± 0.01	51.9 ± 0.9	51.6 ± 0.7
U high-silica melt (ppm)	1.500 ± 0.006	1.9 ± 0.2	1.69 ± 0.06
U zero-aged basalt (ppm)	0.52 ± 0.03	0.39 ± 0.04	0.39 ± 0.05
$(^{238}U/^{230}Th)$ high-silica melt	1	1	1.2
$(^{238}U/^{230}Th)$ zero-aged basalt	1.3	8	0.90 ± 0.01
$(^{226}Ra/^{230}Th)$ high-silica melt	1	1	1.2
$(^{226}Ra/^{230}Th)$ zero-aged basalt	2.9 ± 0.2	17	2.3 ± 0.1

Errors are given at the 1σ level.

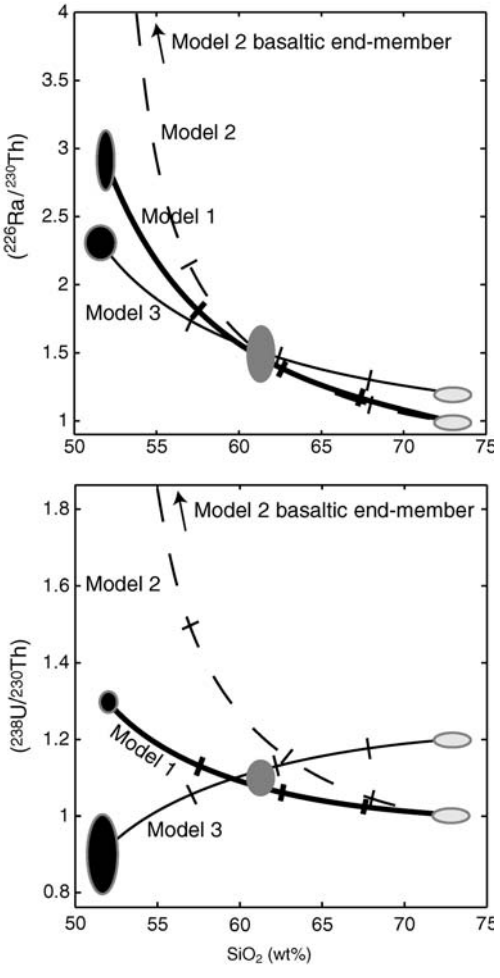

Fig. 1. ($^{238}U/^{230}Th$) and ($^{226}Ra/^{230}Th$) v. SiO_2 (in wt%) mixing diagrams. The composition of the different end-members is shown: in black, zero-age basalt; in light grey, silicic melt derived from lower crust melting. Compositions are shown for the three different models as explained in the text. Tick marks show proportions of zero-age basalt in 25% intervals. It can be seen that the silica composition of the end-members and the proportion of zero-age basalt required to explain the average composition of subduction-related andesites and dacites (dark grey area) do not vary significantly from one model to another (see text for details).

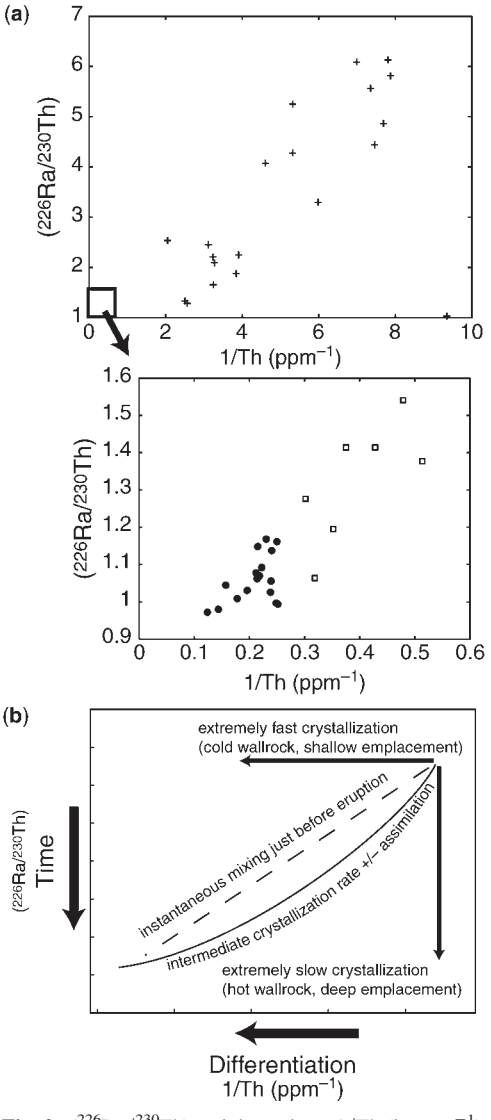

Fig. 2. ($^{226}Ra/^{230}Th$) activity ratio v. 1/Th (in ppm^{-1}) diagram. (**a**) Positive trends are commonly observed for arc lavas: Tonga (crosses; Turner *et al.* 2001); Mount St Helens (squares; Volpe & Hammond 1991); Ruapehu, New Zealand (dots; Price *et al.* 2007). (**b**) Schema showing the effect of crystallization at various rates and mixing in a ($^{226}Ra/^{230}Th$) v. 1/Th diagram.

that the U-series composition of minerals may be complex to interpret (Zellmer *et al.* 2000; Cooper & Reid 2003).

The variation of the mass of magma in the chamber with time is:

$$\frac{dM}{dt} = -f \cdot M + Q_{\text{assimil}} \quad (1)$$

where f is the crystallization rate (in year^{-1}) and Q_{assimil} is the rate of wallrock assimilation (in g year^{-1}). We use the non-dimensional parameter r defined by DePaolo (1981): $r = \frac{Q_{\text{assimil}}}{f \cdot M}$ so that Equation 1 becomes

$$\frac{dM}{dt} = f \cdot M \cdot (r - 1). \quad (2)$$

The variation with time of the mass of a nuclide in the magma, M_i, is

$$\frac{dM_i}{dt} = C_i \cdot \frac{dM}{dt} + M \cdot \frac{dC_i}{dt}$$
$$= r \cdot f \cdot M \cdot C_{i,\text{assimil}} - f \cdot D_i \cdot M \cdot C_i$$
$$+ \lambda_{i-1} \cdot M \cdot C_{i-1} - \lambda_i \cdot M \cdot C_i \quad (3)$$

where C_i and C_{i-1} are respectively the concentrations of the nuclide and its parent in the magma (in g g^{-1}), $C_{i,\text{assimil}}$ the concentration of the nuclide in the assimilated wallrock (in g g^{-1}), D_i the partition coefficient of the nuclide and λ_i and λ_{i-1} are respectively the decay constants of the nuclide and its parent (in year^{-1}).

We can re-write Equation 3 so that:

$$\frac{dC_i}{dt} = r \cdot f \cdot C_{i,\text{assimil}} - C_i \cdot f(r + D_i - 1)$$
$$+ \lambda_{i-1} \cdot C_{i-1} - \lambda_i \cdot C_i. \quad (4)$$

This equation can be written for each nuclide (^{238}U, ^{230}Th, ^{226}Ra and ^{232}Th) and integrated so the evolution of activity ratios with time can be calculated.

The initial composition of the magma is assumed to be similar to the most primitive composition observed: $\text{Th}_i = 1.7$ μg g^{-1} and $(^{226}\text{Ra}/^{230}\text{Th})_i = 1.6$. The composition of the wallrock assimilated is assumed to be: $\text{Th}_{\text{crust}} = 5$ μg g^{-1} and $(^{226}\text{Ra}/^{230}\text{Th})_{\text{crust}} = 1$. Bulk partition coefficients used are 10^{-5} for Ra (Blundy & Wood 2003) and 10^{-2} for Th (for a mineralogical assemblage containing 10% clinopyroxene, which controls Th partitioning; Bacon & Druitt 1988).

If no assimilation occurs ($r=0$), it is possible to reproduce the positive trend observed between (^{226}Ra/^{230}Th) and 1/Th for Mount St Helens and infer that it took about 2000–2500 years for the magma to evolve from the most primitive to the most evolved compositions (Fig. 3). Note that we aim to reproduce the broad trend defined by the data and not each sample composition separately. This timescale is within the range of crystallization ages obtained by Cooper & Reid (2003) for plagioclase (*c.* 2–4 ka) and pyroxene (*c.* 0.15–5.7 ka) in the St Helens lavas. The positive trend defined by the data is best reproduced for a crystallization rate of *c.* $2–3 \times 10^{-4}$ year^{-1}, which is comparable to that inferred from similar data from a number of volcanic systems from a diverse

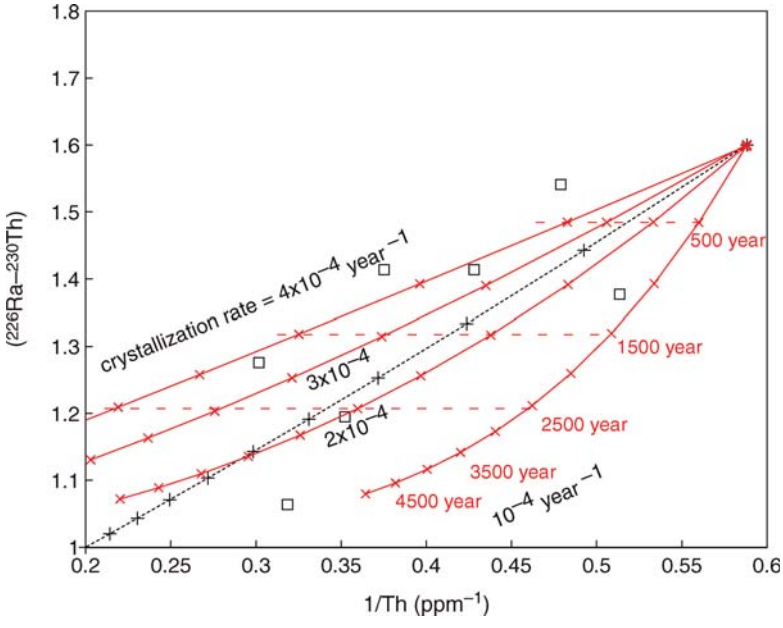

Fig. 3. Closed system fractionation models for Mt St Helens. Squares are wholerock data from Volpe & Hammond (1991). Curves show the evolution of magma composition for different crystallization rates, assuming no crustal assimilation. The magma is assumed to have the following starting composition: Th=1.7 ppm; (^{226}Ra/^{230}Th)=1.6. Partition coefficients used are: $D_{\text{Th}}=0.01$ for Th and $D_{\text{Ra}}=10^{-5}$ for ^{226}Ra. The dotted line shows the effect of instantaneous mixing before eruption between the mafic magma and a crustal melt, with tick marks showing proportions of crustal melt in 10% intervals. The following composition is assumed for the crustal melt: Th=5 ppm; (^{226}Ra/^{230}Th)=1.

range of tectonic settings (Blake & Rogers 2005). As shown in Figure 3, higher crystallization rates produce curves with more gentle slopes than the best fit to the observed trend.

Figure 4 shows that, if assimilation of a secular equilibrium crustal melt accompanies crystal fractionation (AFC), the time inferred to produce the most differentiated magma is significantly reduced (in other words the 'true' time would be overestimated if assimilation was not taken into account). For a ratio of assimilation to crystallization rate (r) of 0.3, suggested to be the highest value yet inferred (Tegner *et al.* 2005), the true timescale for differentiation is reduced to *c.* 1500 years (Fig. 4). As discussed for model I above, in the extreme case of two-end-member mixing, the timescale for differentiation approaches zero. As the rate of assimilation increases relative to crystallization, the inferred timescale for differentiation required to account for the Ra–Th disequilibrium decreases. This is not to say that increasing assimilation leads to faster differentiation. Rather, the timescale inferred from U-series isotopes increasingly overestimates the true timescale as the amount of assimilation increases *if* this effect is not taken into account in the interpretation. Glazner (2007) suggested that wallrock assimilation would increase the crystallization rate. In this case, if $r=0.3$ and the crystallization rate, f, increases from 2 to 4×10^{-4} year^{-1} during AFC, the most silicic composition is produced after *c.* 2000 years (not shown) instead of *c.* 1500 years if f is kept constant and equal to 3×10^{-4} year^{-1}.

The role of amphibole

Davidson *et al.* (2007) have recently shown that the REE composition of arc volcanics indicates an important role for amphibole fractionation in generating the diversity of arc magma geochemistry. Radium can be relatively compatible in amphibole (Blundy & Wood 2003) and so fractionation of amphibole-rich assemblages (or the presence of amphibole as a residual phase during the production of partial melts in the lower crust) could also influence (^{226}Ra/^{230}Th) ratios. Thus, we have also investigated AFC models in which amphibole is a major fractionating phase. The partition coefficient for Ba in amphibole can be up to 0.7 (LaTourrette *et al.* 1995), and assuming that $D_{Ra}=0.08\times D_{Ba}$ (Blundy & Wood 2003), the highest predicted D_{Ra} is 0.056. As Figure 5 shows, because Ra remains relatively incompatible even in amphibole-dominated assemblages, the effect on the inferred timescales is relatively modest (<5%).

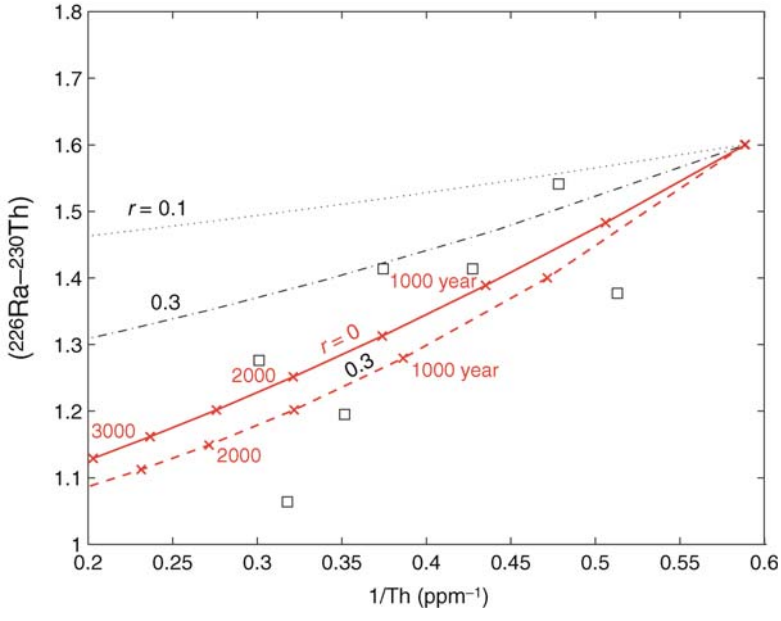

Fig. 4. The effect of crustal assimilation on the evolution of magma composition and comparison with Mount St Helens data. The two upper curves are calculated for different ratios of assimilation over crystallization rates, r (labels on curves), and assuming a crystallization rate infinite compared with ^{226}Ra half-life. The plain and dashed curves are calculated for $r=0$ and 0.3, respectively, and with a crystallization rate of 3×10^{-4} year^{-1} (see Fig. 3). Labels on curve are durations of differentiation. Same symbols, partition coefficients and composition as in Figure 3.

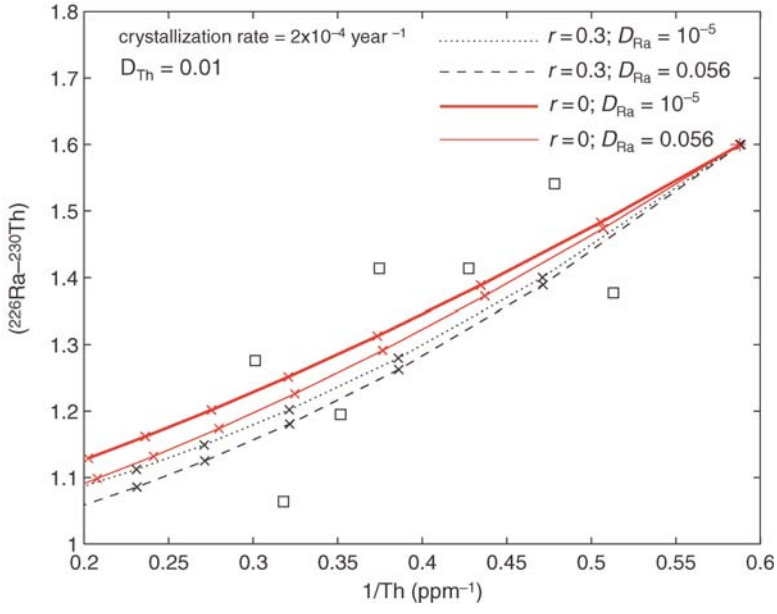

Fig. 5. Dashed and plain curves are calculated on the assumption that amphibole controls ^{226}Ra abundance in the melt. Even if amphibole is an important phase during magma evolution, it can be seen that it does not greatly affect the (^{226}Ra/^{230}Th) of the magma. The composition for the crystallizing magma and the crustal melt are as in Figures 2 & 3. Tick marks on curves are at 500 year intervals.

The effect of recharge

The models above assume no recharge of the magma chamber. Hughes & Hawkesworth (1999) have shown that this process can buffer the decay of ^{226}Ra. In a model of assimilation-recharge-fractional crystallization (ARFC), a primitive magma undergoes fractional crystallization with or without synchronous wallrock assimilation until a new batch of magma is added to the differentiating magma. New batches of magma are added periodically and mixed instantaneously with the resident magma. An equivalent mass of magma is erupted subsequent to this mixing in order to maintain a constant magma volume. Between each recharge event, fractional crystallization occurs with or without wallrock assimilation. Figure 6 shows that the periodic injection of a mass of primitive magma equivalent to 10% of the total mass of magma in the chamber every 500 years slightly increases the time required to produce silicic magmas. In the case of Mount St Helens, the inferred timescale for differentiation increases from *c*. 2000–2500 years (no recharge) to *c*. 2500–3000 years (with recharge) (Fig. 6). A significant increase in the inferred timescales would require larger volumes of replenishing magma. If more frequent recharge is invoked, a steady-state composition with a relatively low Th concentration would be reached and the composition of the most evolved sample cannot be reproduced. It is worth noting that, if crustal assimilation and magma recharge occured concurrently, the resulting timescale for differentiation could be similar to that obtained for the simplest case where closed-system differentiation occurs (i.e. the effects of recharge and assimilation have opposite effects upon disequilibria). In the example of Mount St Helens, assuming the magma recharge scenario and crustal assimilation at a rate 10 times slower that of crystallization (i.e. r=0.1), the time required to produce the most silicic compositions is *c*. 2500 years, similar to the timescale inferred when neither recharge or crustal assimilation occur.

Physical implications

The timescale for differentiation inferred in the previous sections can, in principle, be used to place physical constraints on the depth of differentiation for a given geotherm and magma chamber volume and shape. For Mount St Helens (and other volcanoes such as Ruapehu and Sangeang Api), because differentiation and cooling appear to be fast (<2.5 ka), the magma body is likely to be small and/or located at shallow depths. This can be quantitatively constrained using a cooling

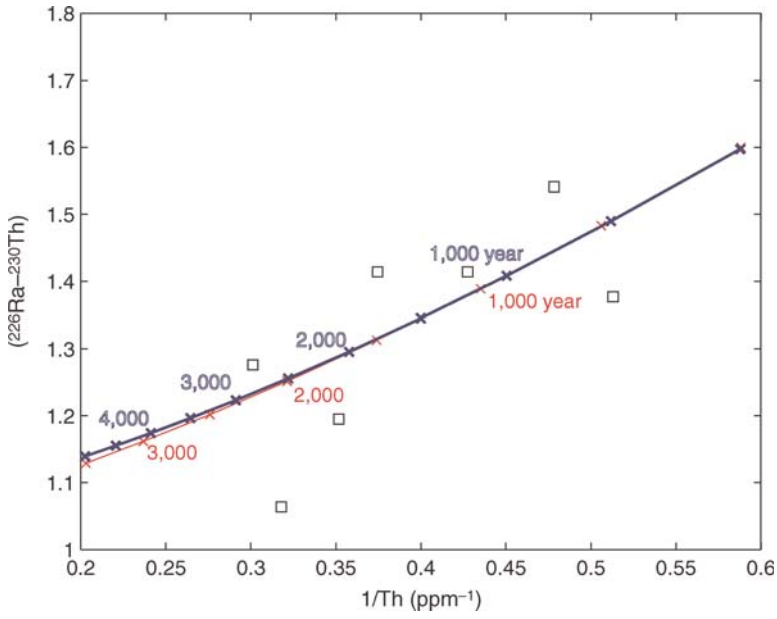

Fig. 6. Magma recharge increases the inferred timescale for differentiation. In the case of Mount St Helens (squares), whereas it takes *c*. 2000–2500 years to produce the most silicic compositions without magma recharge (plain curve), it takes *c*. 2500–3000 years when 10 wt% of primitive magma is added every 500 years (bold curve). The composition of the primitive magma considered is: [Th]=1.7 ppm; (^{226}Ra/^{230}Th)=1.6. The crystallization rate between each magma addition is 3×10^{-4} year^{-1}. Tick marks on curves are at 500 year intervals. Same partition coefficients as in Fig. 3.

model. We model the crystallization of a cooling magma body emplaced instantaneously at a temperature T_{int}, into isothermal crust at a temperature T_{wr}. Our crystallization model is an analytical fit to the crystallization model compiled by Hawkesworth *et al.* (2000) (Fig. 7). We express the crystal mass fraction rate as

$$\frac{\exp\left(-\frac{(T_{int}-T_{trans})^2}{\Delta T^2}\right)}{\sqrt{\pi\Delta T^2}}$$

where the initial temperature of the magma body, T_{int}=1200 °C (Yoder & Tilley 1962), the temperature at which 50% crystallization is achieved, T_{trans}=1137 °C and ΔT=63 °C. Figure 7 shows that this parameter set fits well with the Hawkesworth *et al.* (2000) model, at least up to 85% cumulative crystallization.

We calculate the cooling history of the magma body by solving the thermal energy balance in a spherical coordinate system, using the Finite element package COMSOL. We use a latent heat of crystallization of 400 kJ kg^{-1}, a thermal conductivity of 3 W m^{-1} °C^{-1}, a heat capacity of 1 kJ kg^{-1} °C^{-1} and a density of 2800 kg m^{-3}. We assume that the magma body cools simply by conduction. Convective cooling would not dramatically affect the inferred cooling/crystallization history, since similar timescales are obtained in models where convective heat flux is explicitly taken into account (Hawkesworth *et al.* 2000). Calculations were performed for different aspect ratios, AR=diameter/thickness (AR = 1, spherical magma body; AR>1, oblate-spheroidal magma body, i.e. sheet-like shape; AR<1, prolate-spheroidal magma body, i.e. bottle-shaped) since some workers have argued that magma bodies have a high aspect ratio (Petford *et al.* 2000), although various observations of spherical or prolate-spheroidal intrusions have also been made (Iyer 1984; Marsh 1989; Higgins 1996; Husen *et al.* 2004; Iverson *et al.* 2006; Voight *et al.* 2006). The results are summarized in Figures 8 & 9. Note that similar results are obtained whether we consider a spherical (AR=1) or prolate-spheroidal (AR=0.5) magma body. It is likely that the volume and shape of magma bodies vary for each volcanic centres. For this reason, we again use Mount St Helens to illustrate the approach.

For Mount St Helens, geophysical studies suggest that the magma chamber has an aspect

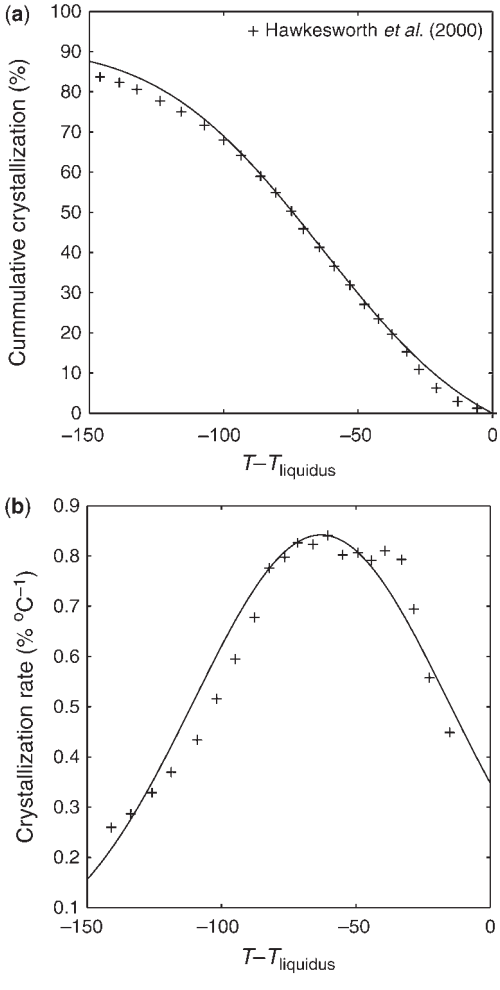

Fig. 7. (**a**) Cumulative crystallization (in %) and (**b**) crystallization rate (in $\%^{\circ}C^{-1}$) as a function of cooling below liquidus used in our thermal models. We use a simple analytical approximation (solid line) fitted to the model of Hawkesworth *et al.* (2000), shown in crosses.

ratio <1 (e.g. Pallister *et al.* 1992; Iverson *et al.* 2006). For AR=0.5, calculations suggest that crystallization of 50% of a magma body >5 km^3 is achieved in *c*. 2000 years (see the previous section) if the wallrock temperature is <500 °C (Fig. 8a). Assuming a geothermal gradient of 30 °C km^{-1}, this corresponds to an emplacement depth <17 km. These are maximum values since at convergent margins the geothermal gradient is often higher than 30 °C km^{-1}, especially if the crust has been heated by repetitive magma intrusions (cf. Annen *et al.* 2006). To produce andesitic and dacitic compositions in the lower crust ($T_{wr} \geq 700$ °C) would require a very small magma

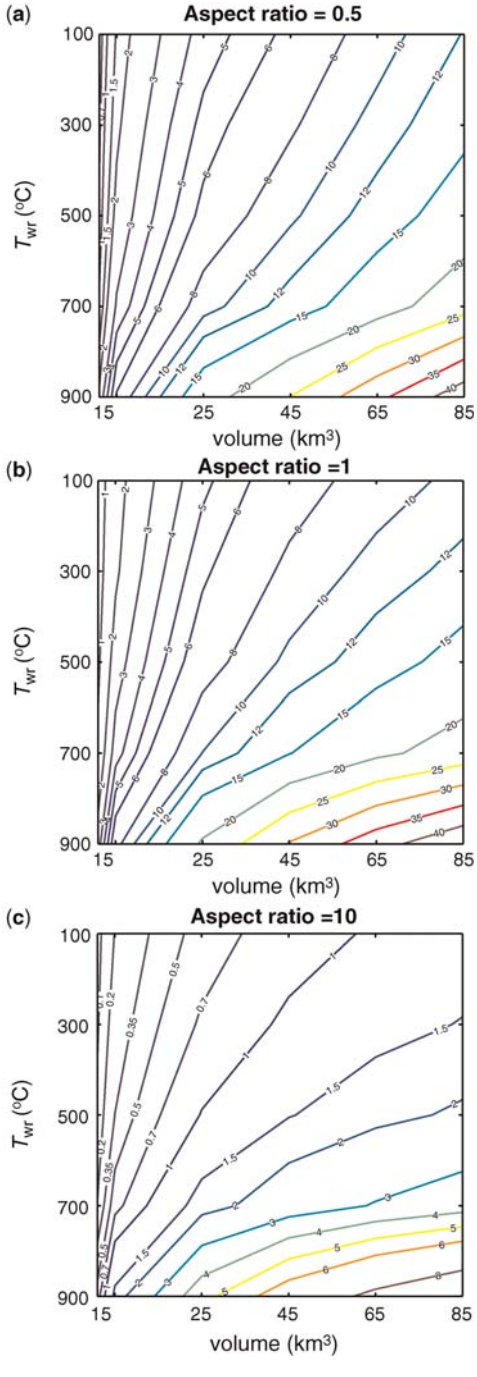

Fig. 8. Curves are isochrons (contoured in ka) showing the time required to precipitate 50% of crystals in (**a**) a prolate spheroidal magma body (aspect ratio=0.5), (**b**) a spherical magma body and (**c**) an oblate spheroidal magma body (aspect ratio=10) for variable magma volumes (*x*-axis) and temperatures of the intruded wallrock (in °C; *y*-axis).

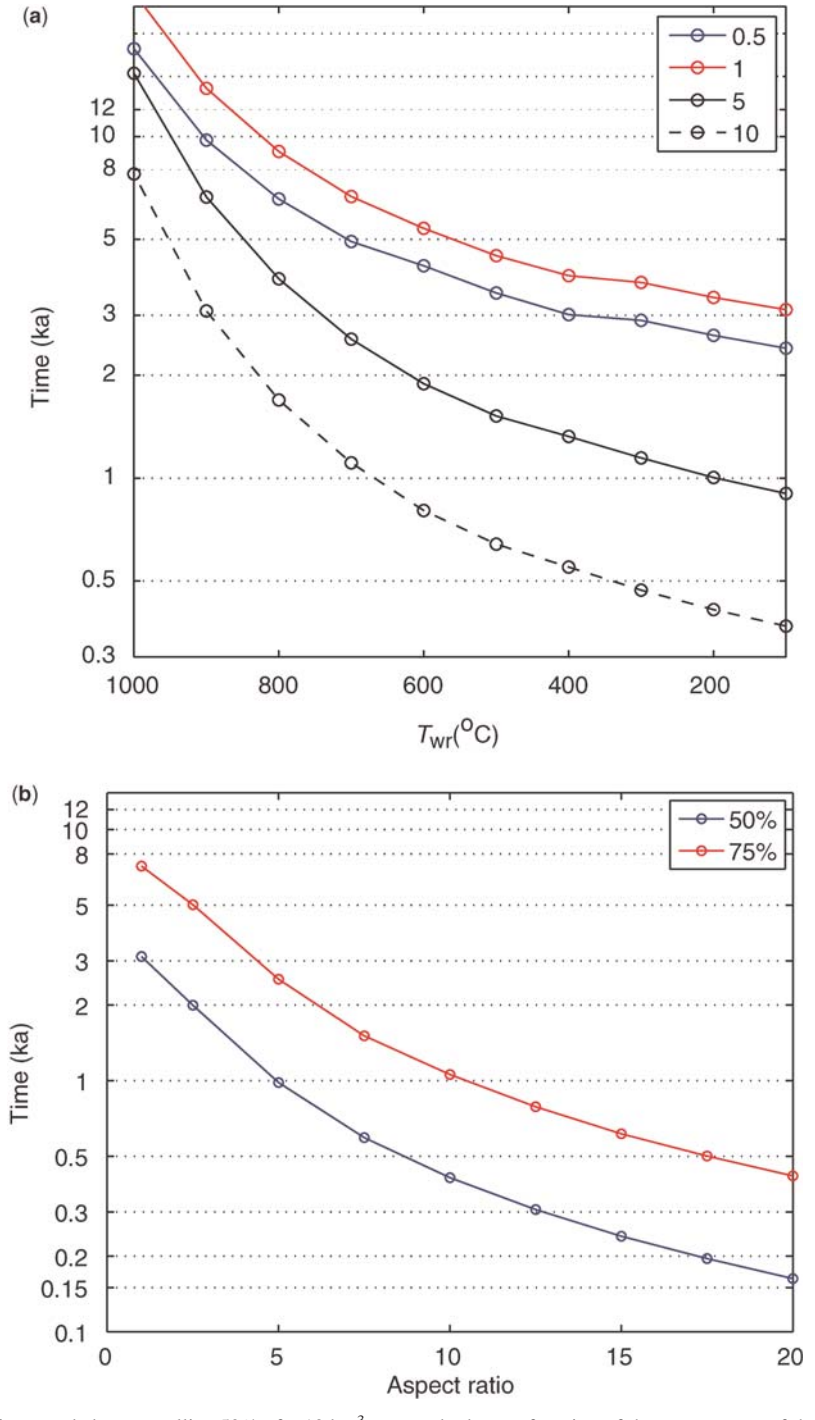

Fig. 9. (**a**) Time needed to crystallize 50% of a 10 km^3 magma body as a function of the temperature of the intruded wallrock T_{wr} (in °C). Curves are shown for magma body aspect ratio=0.5, 1, 5 and 10. (**b**) Time required for the crystallization of a 10 km^3 magma body emplaced in a crust at 300 °C as a function of the magma body aspect ratio. Curves are shown for crystal content=50 and 75%.

body (<3 km^3), which is unlikely (Pallister *et al.* 1992). Hence, our calculations suggest that at Mount St Helens geochemical diversity is produced in the upper crust.

Davidson *et al.* (2007) identified amphibole as a crucial phase during magma chemical evolution. Amphibole can be stable in water-saturated basaltic or andesitic melts at pressures as low as 3 kbar (Beard & Lofgren 1991). Thus, in order to reconcile our cooling model with the stability field of amphibole, differentiation at Mount St Helens must occur in the lowermost pressures of the amphibole stability field (3 kbar). This would correspond to a depth of *c.* 10 km, which is in good agreement with previous geophysics and petrology studies (Lees 1992; Moran 1994; Blundy & Cashman 2005; Iverson *et al.* 2006). In turn, this implies that the size of the magma body is *c.* 10 km^3, since a larger body would require shallower emplacement, incompatible with amphibole stability. This is also in agreement with previous estimates (5–7 km^3; Pallister *et al.* 1992).

The results are remarkably sensitive to magma body shape. For example, a magma volume of 50 km^3 with aspect ratio of 10 (i.e. an oblate spheroidal body with a radius of 5 km and a thickness of 1 km) can undergo 50% crystallization in less than a few thousand years with a wallrock temperature as high as 700 °C. Hence, the ability to constrain the shape of magma bodies at a volcanic centre will be important in attempts to determine whether silicic magmas are produced in shallow spherical or prolate spheroidal magma bodies (e.g. Mount St Helens, Pallister *et al.* 1992; Mount Taranaki, New Zealand, Higgins 1996) or deep oblate spheroidal bodies (i.e. sheet-like sills).

Finally, we note that other processes can potentially yield extremely short differentiation timescales. For instance, Blundy & Cashman (2005) argued that crystallization can be driven by (rapid) decompression and degassing. However, whether this could occur over thousands of years as indicated by the Ra–Th disequilibria data remains to be shown.

Conclusions

We have quantitatively investigated several end-member models to account for the uranium-series isotopic variation often observed in co-genetic suites of andesites and dacites and used these to explore time and space constraints on the processes responsible for their generation. In the first model, the composition of silicic magmas is assumed to result solely from mixing between residual melts from differentiation and crustal melting with zero-aged basalt shortly before eruption. The results suggest that about half of the erupted magma volume has to be derived from crustal and residual melts. Considering the few case studies in which pure two end-member mixing has been established, this scenario is deemed unlikely. In the second model, primary basalt and crustal melts are mixed during differentiation (AFC) rather than just before eruption (first model), and Ra–Th data from Mount St Helens are used as a case study to quantify the effect of crustal assimilation on inferred differentiation timescales. Crustal assimilation during crystallization reduces (^{226}Ra/^{230}Th) more rapidly than the effect of the passage of time alone. Including amphibole as a major crystallizing phase also decreases (^{226}Ra/^{230}Th) ratios but this effect is not dramatic. Thus, all of the processes considered here lead to reductions in the timescales of differentiation that have been inferred from negative (^{226}Ra/^{230}Th) – Th arrays assuming crystal fractionation was the only processes operating. Consequently, the timescales inferred from such studies should be considered as maxima. Frequent magma recharge can increase the inferred timescales of differentiation. However, this effect is significant only if large amounts of primitive magma frequently replenish the chamber (>20 wt% of the magma in the chamber every 500 years). Because of the short timescales inferred, simple thermal models for magma cooling may require that differentiation occurs shallowly, depending on magma chamber geometry. By combining this with the suggestion that amphibole was an important crystallizing phase (Davidson *et al.* 2007), we infer that magma emplacement below Mount St Helens occurred at a depth of *c.* 10 km and that the size of the magma body is *c.* 10 km^3. This is consistent with recent geodetic data (Iverson *et al.* 2006). Hence, production of silicic magma in spherical or prolate spheroidal (i.e. bottle-shaped) magma bodies probably occurs in the mid-upper crust. Oblate spheroidal magma bodies (i.e. sheet-like sills) can cool over shorter timescales (a few thousand years) at deeper depths. Future studies combining geophysical imagery and geochemical tools such as U-series isotopes at other volcanic centres should provide important constraints on the mechanisms and locations of silicic magma production.

We would like to thank T. Rushmer and C. O'Neill for helpful discussions. We would also like to thank the editor (C. Annen) and the reviewers (G. Zellmer and Ch. Hawkesworth) for their helpful comments that largely improved the manuscript. S.P.T. acknowledges an ARC Federation Fellowship. This research was funded by ARC grant DP0451704. This is GEMOC publication no. 507.

References

ANNEN, C., BLUNDY, J. D. & SPARKS, R. S. 2006. The genesis of intermediate and silicic magmas in deep crustal hot zones. *Journal of Petrology*, **47**, 505–539.

ANNEN, C. & SPARKS, R. S. J. 2002. Effects of repetitive emplacement of basaltic intrusions on thermal evolution and melt generation in the crust. *Earth and Planetary Science Letters*, **203**, 937–955.

BACON, C. R. & DRUITT, T. H. 1988. Compositional evolution of the zoned calcalkaline magma chamber of Mount-Mazama, Crater Lake, Oregon. *Contributions to Mineralogy and Petrology*, **98**, 224–256.

BEARD, J. S. & LOFGREN, G. E. 1991. Dehydration melting and water-saturated melting of basaltic and andesitic greenstones and amphibolites at 1, 3, and 6.9 kb. *Journal of Petrology*, **32**, 365–401.

BERGANTZ, G. W. 1989. Underplating and partial melting: implications for melt generation and extraction. *Science*, **245**, 1093–1095.

BERGANTZ, G. W. & DAWES, R. 1992. Aspects of magma generation and ascent in continental lithosphere. *In*: RYAN, M. P. (ed.) *Magmatic Systems*. Academic Press, San Diego, CA, 291–317.

BERLO, K., TURNER, S., BLUNDY, J. & HAWKESWORTH, C. 2004. The extent of U-series disequilibria produced during partial melting of the lower crust with implications for the formation of the Mount St. Helens dacites. *Contributions to Mineralogy and Petrology*, **148**, 122–130.

BLAKE, S. & ROGERS, N. 2005. Magma differentiation rates from (^{226}Ra–^{230}Th) and the size and power output of magma chambers. *Earth and Planetary Science Letters*, **236**, 654–669.

BLUNDY, J. & CASHMAN, K. 2005. Rapid decompression-driven crystallization recorded by melt inclusions from Mount St. Helens volcano. *Geology*, **33**, 793–796.

BLUNDY, J. & WOOD, B. 2003. Mineral-melt partition of Uranium, Thorium and their daughters. *In*: BOURDON, B., HENDERSON, G. M., LUNDSTROM, C. C. & TURNER, S. P. (eds) *Uranium-series Geochemistry*. Geochemical Society, Mineralogical Society of America, Washington, DC, **52**, 59–123.

BOURDON, B., WÖRNER, G. & ZINDLER, A. 2000. U-series evidence for crustal involvement and magma residence times in the petrogenesis of Parinacota volcano, Chile. *Contributions to Mineralogy Petrology*, **139**, 458–469.

BOURDON, B., TURNER, S. & DOSSETO, A. 2003. Dehydration and partial melting in subduction zones: constraints from U-series disequilibria. *Journal of Geophysical Research B: Solid Earth*, ECV 3-1–3-19.

COOPER, K. M. & REID, M. R. 2003. Re-examination of crystal ages in recent Mount St. Helens lavas: implications for magma reservoir processes. *Earth and Planetary Science Letters*, **213**, 149–167.

DAVIDSON, J. 1985. Mechanisms of contamination in Lesser Antilles island arc magmas from radiogenic and oxygen isotope relationships. *Earth and Planetary Science Letters*, **72**, 163–174.

DAVIDSON, J., TURNER, S., HANDLEY, H., MACPHERSON, C. & DOSSETO, A. 2007. An amphibole "sponge" in arc crust? *Geology*, **35**, 787–790.

DEPAOLO, D. J. 1981. Trace element and isotopic effects of combined wallrock assimilation and fractional crystallization. *Earth and Planetary Science Letters*, **53**, 189–202.

DOSSETO, A., BOURDON, B., JORON, J.-L. & DUPRÉ, B. 2003. U–Th–Pa–Ra study of the Kamchatka arc: new constraints on the genesis of arc basalts. *Geochimica et Cosmochimica Acta*, **67**, 2857–2877.

DUFEK, J. & COOPER, K. M. 2005. ^{226}Ra/^{230}Th excess generated in the lower crust: Implications for magma transport and storage timescales. *Geology*, **33**, 833–836.

GEORGE, R., TURNER, S., HAWKESWORTH, C., BACON, C. R., NYE, C., STELLING, P. & DREHER, S. 2004. Chemical versus temporal controls on the evolution of tholeiitic and calc-alkaline magmas at two volcanoes in the Alaska–Aleutian Arc. *Journal of Petrology*, **45**, 203–219.

GLAZNER, A. F. 2007. Thermal limitations on incroporation of wall rock into magma. *Geology*, **35**, 319–333.

GROVE, T. L. & KINZLER, R. J. 1986. Petrogenesis of andesites. *Annual Review of Earth and Planetary Sciences*, **14**, 417–454.

GROVE, T. L., KINZLER, R. J., BAKER, M. B., DONNELLY-NOLAN, J. M. & LESHER, C. E. 1988. Assimilation of granite by basaltic magma at Burnt Lava Flow, Medicine Lake Volcano, Northern California – decoupling of heat and mass-transfer. *Contributions to Mineralogy and Petrology*, **99**, 320–343.

HALLIDAY, A. N., FALLICK, A. E., DICKIN, A. P., MACKENZIE, A. B., STEPHENS, W. E. & HILDRETH, W. 1983. The isotopic and chemical evolution of Mount St. Helens. *Earth and Planetary Science Letters*, **63**, 241–256.

HAWKESWORTH, C. J., BLAKE, S., EVANS, P., HUGHES, R., MACDONALD, R., THOMAS, L. E., TURNER, S. P. & ZELLMER, G. 2000. Time scales of crystal fractionation in magma chambers – integrating physical, isotopic and geochemical perspectives. *Journal of Petrology*, **41**, 991–1006.

HIGGINS, M. D. 1996. Crystal size distributions and other quantitative textural measurements in lavas and tuff from Egmont volcano (Mt. Taranaki), New Zealand. *Bulletin of Volcanology*, **58**, 194–204.

HUGHES, R. D. & HAWKESWORTH, C. J. 1999. The effects of magma replenishment processes on ^{238}U–^{230}Th disequilibrium. *Geochimica et Cosmochimica Acta*, **63**, 4101–4110.

HUPPERT, H. E. & SPARKS, R. S. 1988. The generation of granitic magmas by intrusion of basalt into the continental crust. *Journal of Petrology*, **29**, 599–624.

HUSEN, S., SMITH, R. B. & WAITE, G. P. 2004. Evidence for gas and magmatic sources beneath the Yellowstone volcanic field from seismic tomographic imaging. *Journal of Volcanology and Geothermal Research*, **131**, 397–410.

IVERSON, R. M., DZURISIN, D. *ET AL.* 2006. Dynamics of seismogenic volcanic extrusion at Mount St Helens in 2004–05. *Nature*, **444**, 439–443.

IYER, H. M. 1984. Geophysical evidence for the locations, shapes and sizes, and internal structures of magma chambers beneath regions of Quaternary volcanism.

Philosophical Transactions of the Royal Society of London. Series A, Mathematical and Physical Sciences, **310**, 473–510.

LATOURRETTE, T., HERVIG, R. L. & HOLLOWAY, J. R. 1995. Trace element partitioning between amphibole, phlogopite, and basanite melt. *Earth and Planetary Science Letters*, **135**, 13–30.

LAUBE, N. & SPRINGER, J. 1998. Crustal melting by ponding of mafic magmas: a numerical model. *Journal of Volcanology and Geothermal Research*, **81**, 19–35.

LEES, J. M. 1992. The magma system of Mount St. Helens: non-linear high-resolution P-wave tomography. *Journal of Volcanology and Geothermal Research*, **53**, 103–116.

MARSH, B. D. 1989. Magma chambers. *Annual Review of Earth Planetary Sciences*, **17**, 439–474.

MORAN, S. C. 1994. Seismicity at Mount St. Helens, 1987–1992: evidence for repressurization of an active magmatic system. *Journal of Geophysical Research*, **99**, 4341–4354.

OROZCO-ESQUIVEL, M. T., NIETO-SAMANIEGO, A. F. & ALANIZ-ALVARES, S. A. 2002. Origin of rhyolitic lavas in the Mesa Central, Mexico, by crustal melting related to extension. *Journal of Volcanology and Geothermal Research*, **118**, 37–56.

PALLISTER, J. S., HOBLITT, R. P., CRANDELL, D. R. & MULLINEAUX, D. R. 1992. Mount St Helens a decade after the 1980 eruptions: magmatic models, chemical cycles, and a revised hazards assessment. *Bulletin of Volcanology*, **54**, 124–146.

PETFORD, N. & GALLAGHER, K. 2001. Partial melting of mafic (amphibolitic) lower crust by periodic influx of basaltic magma. *Earth and Planetary Science Letters*, **193**, 483–499.

PETFORD, N., CRUDEN, A. R., MCCAFFREY, K. J. W. & VIGNERESSE, J.-L. 2000. Granite magma formation, transport and emplacement in the Earth's crust. *Nature*, **408**, 669–673.

PRICE, R. C., GEORGE, R. *ET AL*. 2007. U–Th–Ra fractionation during crustal-level andesite formation at Ruapehu volcano, New Zealand. *Chemical Geology*, **244**, 437–451.

SMITH, D. R. & LEEMAN, W. P. 1987. Petrogenesis of Mount St. Helens dacitic magmas. *Journal of Geophysical Research*, **92**, 10313–10334.

SPARKS, R. S. J. & MARSHALL, L. A. 1986. Thermal and mechanical constraints on mixing between mafic and silicic magmas. *Journal of Volcanology and Geothermal Research*, **29**, 99–124.

TAYLOR, S. R. & MCLENNAN, S. M. 1995. The geochemical evolution of the continental crust. *Reviews in Geophysics*, **33**, 241–265.

TEGNER, C., WILSON, J. R. & ROBINS, B. 2005. Crustal assimilation in basalt and jotunite: constraints from layered intrusions. *Lithos*, **83**, 299–316.

TEPPER, J. H., NELSON, B. K., BERGANTZ, G. W. & IRVING, A. J. 1993. Petrology of the Chiilwack batholith, North Cascades, Washington. Generation of calc-alkaline granitoids by melting of mafic lower crust with variable water fugacity. *Contributions to Mineralogy and Petrology*, **113**, 333–351.

TURNER, S., EVANS, P. & HAWKESWORTH, C. 2001. Ultrafast source-to-surface movement of melt at island arcs from 226Ra-230Th systematics. *Science*, **292**, 1363–1366.

TURNER, S., BOURDON, B. & GILL, J. 2003*a*. Insights into magma genesis at convergent margins from U-series isotopes. *In*: BOURDON, B., HENDERSON, G. M., LUNDSTROM, C. C. & TURNER, S. P. (eds) *Uranium-Series Geochemistry*. Geochemical Society, Mineralogical Society of America, Washington, DC, **52**, 255–315.

TURNER, S., FODEN, J., GEORGE, R., EVANS, P., VAME, R., ELBURG, M. & JENNER, G. 2003*b*. Rates and processes of potassic magma generation at Sangeang Api volcano, east Sunda arc, Indonesia. *Journal of Petrology*, **44**, 491–515.

VOIGHT, B., LINDE, A. T. *ET AL*. 2006. Unprecedented pressure increase in deep magma reservoir triggered by lava-dome collapse. *Geophysical Research Letters*, **33**, L03312.

VOLPE, A. M. & HAMMOND, P. E. 1991. ^{238}U–^{230}Th—^{226}Ra disequilibria in young Mount St. Helens rocks: time constraint for magma formation and crystallization. *Earth and Planetary Science Letters*, **107**, 475–486.

YODER, H. S., JR & TILLEY, C. E. 1962. Origin of basalt magmas: an experimental study of natural and synthetic rock systems. *Journal of Petrology*, **3**, 342–532.

ZELLMER, G., TURNER, S. & HAWKESWORTH, C. 2000. Timescales of destructive plate margin magmatism: new insights from Santorini, Aegean volcanic arc. *Earth and Planetary Science Letters*, **174**, 265–281.

ZELLMER, G. F., ANNEN, C., CHARLIER, B. L. A., GEORGE, R. M., TURNER, S. P. & HAWKESWORTH, C. J. 2005. Magma evolution and ascent at volcanic arcs; constraining petrogenetic processes through rates and chronologies. *Journal of Volcanology and Geothermal Research*, **140**, 171–191.